Original Research Article

Numerical simulations of a population dynamic model describing parasite destruction in a wild type pine forest

Pierre Magal [a,b,*], Zhengyang Zhang [a,b]

[a] Univ. Bordeaux, IMB, UMR 5251, F-33400 Talence, France
[b] CNRS, IMB, UMR 5251, F-33400 Talence, France

ABSTRACT

We consider a population dynamic model describing the growth of wild pine tree forest. This type of model incorporates the demography of the tree population (i.e. reproduction and death of trees), and also incorporates a maturation time that depends on the number of adult trees.

The goal of this article is to introduce a parasite called nematode into such a forest. Since this parasite colonizes pine trees to reproduce, it is natural to introduce a predator-prey (or consumer-resource) relationship between the trees and the parasites.

In order to investigate the behaviour of the resulting system, we will use numerical simulations, and we will introduce a parasite into a population of trees that: (1) is not oscillating around the positive equilibrium; (2) has some damped oscillations; (3) has some undamped oscillations. This will correspond to three scenarios for parameter values. As one may expect, this will lead to complex dynamics, since we combine the oscillations produced by the predator-prey system with the oscillations coming from the demographic properties of the prey.

© 2017 Elsevier B.V. All rights reserved.

1. Introduction

Pine wilt disease (PWD) is one of the most serious disease of pine species in all over the world. The pathogenic agent of PWD is the pine wood nematode (PWN) *Bursaphelenchus xylophilus*, and it is transmitted from tree to tree by a species of insect *Monochamus*. This PWN is a native nematode species in North America. It was first introduced in Japan in the early 20th century and spreaded into other Asian countries (China, Korea, etc.) in the 1980s. In 1999, it was first detected in Portugal (Mota et al., 1999) and its only insect vector in this region was *Monochamus galloprovincialis* (Sousa et al., 2001, 2002). In 2008, with the detection of this PWN in other areas of Portugal and even on Madeira Island, the entire territory of Portugal was affected (Rodrigues, 2008). PWD also spreads into other European countries due to the wood transportation. For more information about the spread of PWD in Europe and in the world, we refer in addition to Mota et al. (2009); Mota and Vieira (2008); Vicente et al. (2012) and the references therein.

In this paper we consider the population of nematode, which is a parasite spreading into a wild pine tree forest. This means that we totally neglect the way the nematode spreads in between the pine trees, namely the insect vector *Monochamus galloprovincialis*. The life cycle of nematode is very short (around 4 days). In comparison, the pine tree's life cycle is rather slow. Therefore it makes sense to use instantaneous production of new nematodes when pine trees are degraded by nematodes and serve as a resource to produce new nematodes. We refer to Koutroumpa (2007) for more information about the biology of nematode.

There have been some attempts to build a model to describe the dynamics in the pine-nematode community (Gruffudd et al., 2016 and the references therein). In this paper, in order to describe the relationship between pine trees and nematodes, we will use a predator-prey system which goes back to Lotka (1925) and Volterra (1927, 1928) in the early 20th century. More generally speaking, the class of system we have in mind is the so-called consumer-resource model which attracts a lot of interests in ecology during the last four decades. We refer to Holland and DeAngelis (2009, 2010); Lafferty et al., (2015); MacArthur (1972); May (1972); Rosenzweig and MacArthur (1963) and the references therein for a nice overview on this subject. Let $A(t)$ be the number of adult pine trees, and $I(t)$ be the number of nematodes. We consider a simpli-

---

fied model for the population dynamics of pine trees and nematodes

$$
\begin{cases}
\dfrac{dA(t)}{dt} = (\beta - \mu_A)A(t) - \dfrac{\gamma_A I(t)A(t)}{1 + \kappa A(t)}, \text{pine tree destruction} \\
\end{cases}
$$

$$
\dfrac{dI(t)}{dt} = \left(\dfrac{\varepsilon \chi \gamma_A A(t)}{1 + \kappa A(t)} \text{production of new nematodes} - \mu_I \right) I(t),
$$
(1.1)

where $\beta > 0$ is the birth rate of trees, $\mu_A > 0$ is the natural mortality of adult trees, $\gamma_A > 0$ is the number of adult trees consumed per nematode per unit time, $\kappa \geqslant 0$ is interpreted as a constant handling time for each prey captured (Accolla, 2015; Dawes and Souza, 2013; Kazarinoff and Driessche, 1978), $\varepsilon > 0$ is the conversion efficiency from tree biomass to nematode biomass, $\chi > 0$ is the birth rate of nematodes, $\mu_I > 0$ is the natural mortality of nematodes.

One may observe that the special case $\kappa = 0$ of system (1.1) corresponds to the classical Lotka-Volterra model, while the case $\kappa > 0$ corresponds to the Holling's type II functional response (Holling, 1959a, 1959b). In the article we will investigate both cases for κ.

In order to incorporate the vital dynamics of the population of trees, we need to add a limitation of the growth of trees due to the competition for light. This can be achieved by using the so-called size-structured models. We refer to Magal and Zhang (2017a); Smith (1993, 1994); Webb (2008) for a nice survey on this topic. In Magal and Zhang (2017a) a comparison of size-structured model with a forest computer simulator has been successfully done, and the model considered takes the following form

$$
\begin{cases}
\partial_t u(t,s) + f(A(t))\partial_s u(t,s) = -\mu(s)u(t,s), \text{ for } t \geq 0, s \geq s_-, \\
f(A(t))u(t,s_-) = \beta A(t), \text{ for } t \geq 0
\end{cases}
$$
(1.2)

with the initial distribution of trees

$$
u(0,.) = u_0(.) \in L^1(0, +\infty),
$$

where $s_- > 0$ is the minimal size of juvenile trees and $s \mapsto u(t,s)$ is the density of population of trees of size s at time t, which means that for each $s_2 \geqslant s_1 \geqslant s_-$,

$$
\int_{s_1}^{s_2} u(t,s)ds
$$

is the number of trees of size in between s_1 and s_2 at time t. Therefore the total number of trees in the population is

$$
U(t) = \int_{s_-}^{+\infty} u(t,s)ds.
$$

We assume that the number of adult and juvenile trees are respectively given by

$$
A(t) := \int_{s^*}^{+\infty} u(t,s)ds \text{ and } J(t) := \int_{s_-}^{s^*} u(t,s)ds
$$

where $s^* > s_-$ is the size of maturity for trees, namely the minimal size of adult trees.

Moreover, to describe the fact that the more adult trees there are, the less light is left to juvenile trees to grow, we assume that the growth speed depends on the number of adults, namely

$$
f(A(t)) := \dfrac{\alpha}{1 + \delta A(t)},
$$

where $\alpha > 0$ and $\delta > 0$ are parameters that will be determined later on.

The full model combining both the parasite destruction and the vital dynamics of the population of tree is the following

$$
\begin{cases}
\partial_t u(t,s) + f(A(t))\partial_s u(t,s) = -\left[\mu(s) + \dfrac{\gamma(s)I(t)}{1 + \kappa A(t)} \right] u(t,s),
\end{cases}
$$

for $s \geq s_-, t \geq 0, \ f(A(t))u(t,s_-) = \beta A(t), \text{ for } t \geq 0, \ \dfrac{dI(t)}{dt}$

$$
= \dfrac{\varepsilon \chi}{1 + \kappa A(t)} \int_{s_-}^{+\infty} \gamma(s)u(t,s)ds I(t)
$$
$$
- \mu_I I(t), \text{ for } t \geq 0,
$$
(1.3)

with the initial distributions

$$
u(0,.) = u_0(.) \in L^1(0, +\infty); \ I(0) = I_0 \geq 0.
$$

In system (1.3) $\mu(s) > 0$ is the mortality of trees of size s and $\gamma(s) \geqslant 0$ is the number of trees of size s consumed per nematode per unit time. We assume for simplicity that

$$
\mu(s) = \begin{cases} \mu_A > 0, & \text{if } s \geq s^*, \\ \mu_J > 0, & \text{if } s < s^*, \end{cases} \quad \gamma(s) = \begin{cases} \gamma_A \geq 0, & \text{if } s \geq s^*, \\ \gamma_J \geq 0, & \text{if } s < s^*. \end{cases}
$$

As is described in Appendix A (see also Magal and Zhang, 2017a; Smith, 1993, 1994), we can transform system (1.3) into the following state-dependent delay differential equations

$$
\begin{cases}
\dfrac{dA(t)}{dt} = f(A(t)) \dfrac{\beta A(t - \tau(t))}{f(A(t - \tau(t)))} e^{-\mu_J \tau(t) - \gamma_J \int_{t-\tau(t)}^t \frac{I(l)}{1 + \kappa A(l)} dl} \\
\qquad - \mu_A A(t) - \dfrac{\gamma_A I(t)A(t)}{1 + \kappa A(t)}, \int_{t-\tau(t)}^t f(A(\sigma))d\sigma = s^* - s_-, \\
\dfrac{dI(t)}{dt} = \left[\dfrac{\varepsilon \chi}{1 + \kappa A(t)} (\gamma_A A(t) + \gamma_J J(t)) - \mu_I \right] I(t),
\end{cases}
$$
(1.4)

with the initial distributions

$$
A(t) = A_0(t) \geq 0, \forall t \in (-\infty, 0]; \ \tau(0) = \tau_0 \geq 0; \ I(0) = I_0 \geq 0.
$$

In system (1.4), the function $\tau(t)$ describes the time needed by a tree to grow to the maturity size s^* at time t from the minimal size s_-. Namely $\tau(t)$ the time needed for a tree to become mature at time t. Then we must have $\tau_0 \geqslant 0$ the initial length of maturation satisfying

$$
\int_{-\tau_0}^0 f(A_0(\sigma))d\sigma = s^* - s_-,
$$

and the second equation of (1.4) is equivalent to

$$
\int_{t-\tau(t)}^t f(A(\sigma))d\sigma = \int_{-\tau_0}^0 f(A_0(\sigma))d\sigma,
$$

where the initial value $\tau(0) = \tau_0$ is derived. Therefore we can fix either $\tau(t)$ at time $t = 0$, or equivalently $s^* - s_-$, which is the difference between the size of maturity s^* and the size at birth s_-. A detailed explanation will also be found in Appendix A.

In the following we will assume for simplicity that $\gamma_A > 0$ and $\gamma_J = 0$. Therefore in this article we consider the following model

$$
\begin{cases}
\dfrac{dA(t)}{dt} = f(A(t)) \dfrac{\beta A(t - \tau(t))}{f(A(t - \tau(t)))} e^{-\mu_J \tau(t)} - \mu_A A(t) - \dfrac{\gamma_A I(t)A(t)}{1 + \kappa A(t)}, \\
\displaystyle\int_{t-\tau(t)}^t f(A(\sigma))d\sigma = \int_{-\tau_0}^0 f(A_0(\sigma))d\sigma, \\
\dfrac{dI(t)}{dt} = \left(\dfrac{\varepsilon \chi \gamma_A A(t)}{1 + \kappa A(t)} - \mu_I \right) I(t)
\end{cases}
$$
(1.5)

with the initial distributions

$$
A(t) = A_0(t) \geq 0, \forall t \in (-\infty, 0]; \ \tau(0) = \tau_0 \geq 0; \ I(0) = I_0 \geq 0.
$$

The first basic fact about system (1.5) is that when $I_0 = 0$ then

$$
I(t) = 0, \forall t \geq 0.
$$

Therefore $I_0 = 0$ corresponds to the model without parasite, namely Eq. (1.2).

Table 1

We show in this table the parameter values used in the numerical simulations of system (1.5). The first six parameter values come from Magal and Zhang (2017a). We set $s_- = 0$ for simplicity and we use the formula $\int_{-\tau_0}^{0} f(A(s))\mathrm{d}s = s^* - s_-$ to calculate s^*. Notice also that with Holling's type II functional response, we will investigate three cases regarding different values of the conversion efficiency $\varepsilon = 0.68$, $\varepsilon = 1$ and $\varepsilon = 10$ for each scenario. Scenario 1-3 correspond to three different dynamics of adult tree population. This will serve to investigate the effect of the introduction of nematodes depending on the type of dynamics of adult tree population.

Parameter	Lotka-Volterra form			Holling's type II functional response		
	Scenario 1	Scenario 2	Scenario 3	Scenario 1	Scenario 2	Scenario 3
μ_J	0.03	0.031	0.0036	0.03	0.031	0.03
μ_A	0.001	0.0037	0.001	0.001	0.0037	0.06
β	2	4	2	2	4	2
δ	0.1	0.1	0.1	0.1	0.1	0.1
α	0.1709	0.249	0.1709	0.1709	0.249	0.1709
τ_0	121	127	121	121	127	121
s_-	0	0	0	0	0	0
s^*	0.5318	0.4164	0.5318	0.5318	0.4164	0.5318
γ_A	0.001	0.001	0.001	0.001	0.001	0.001
κ	0	0	0	0.0001	0.0001	0.0001
ε	1	1	1	0.68/1/10	0.68/1/10	0.68/1/10
χ	0.1	0.1	0.1	0.1	0.1	0.1
μ_I	0.05	0.05	0.05	0.05	0.05	0.05

One can also prove that (see Magal and Zhang, 2017b) when $\tau_0 = 0$ then

$$\tau(t) = 0, \forall t \geq 0.$$

This means that when $\tau_0 = 0$, the system (1.5) becomes (1.1).

The goal of this article is to investigate the influence of introducing nematodes into a pine tree forest population. This can be regarded as a predator-prey system where the prey has (possibly) a complex dynamics describing a state-dependent delay differential equation. We will investigate some scenarios of the tree population and add the parasite into such a population.

The article is organized as follows. In the second section we compute the positive interior equilibrium. In the third section, we will conduct the numerical simulations of system (1.5). We will start by reviewing some "classical" results about the predator-prey model in ODE case (1.1). Then we will conduct some simulations of system (1.5) in several cases and scenarios (see Table 1). We conclude the paper by discussing the numerical results to see what influence the maturation delay and the introduction of nematodes bring to the solutions.

2. Positive interior equilibrium

The system (1.5) has a unique interior equilibrium

$$\bar{A} := \frac{\mu_I}{\varepsilon \chi \gamma_A - \mu_I \kappa}, \bar{\tau} := \frac{s^* - s_-}{f(\bar{A})} \text{ and } \bar{I} := \left(\beta e^{-\mu_J \bar{\tau}} - \mu_A\right)\frac{1 + \kappa \bar{A}}{\gamma_A}.$$

Therefore system (1.5) will have a unique positive interior equilibrium if and only if

$$\varepsilon \chi \gamma_A - \mu_I \kappa > 0 \text{ and } \beta e^{-\mu_J \bar{\tau}} - \mu_A > 0. \tag{2.1}$$

In particular if we assume that $\bar{\tau} = 0$ (i.e. $s^* - s_- = 0$), we obtain a unique positive interior equilibrium for system (1.1) if and only if

$$\varepsilon \chi \gamma_A - \mu_I \kappa > 0 \text{ and } \beta - \mu_A > 0. \tag{2.2}$$

Remark 2.1. Even though we don't know how to investigate analytically the uniform persistence for system (1.5), we strongly suspect that the parasite will persist if and only if the condition (2.1) is satisfied. Therefore one may compare conditions (2.1) and (2.2) to see the effect of the vital dynamics of the tree population on the persistence of parasite.

3. Numerical simulations

In this section we will conduct some numerical simulations of system (1.5). According to the analysis in Magal and Zhang (2017a),

we have two scenarios of population dynamics of adult trees population $A(t)$ without nematodes (namely when $I_0 = 0$): a steady solution (Scenario 1), a damped oscillating solution (Scenario 2). And by changing one parameter μ_J in Scenario 1, we will get a third scenario: a periodic solution (Scenario 3). We list all the parameters used in the numerical simulations for the three scenarios in Table 1 and calculate the positive interior equilibrium in Table 2.

3.1. Model without maturation period – case $\tau = 0$

In this subsection we will review some results about the classical predator-prey ODE system (1.1).

3.1.1. Lotka-Volterra form – case $\kappa = 0$

Set $\kappa = 0$, then system (1.1) becomes the classical Lotka-Volterra model

$$\begin{cases} \dfrac{dA(t)}{dt} = (\beta - \mu_A)A(t) - \gamma_A I(t)A(t), \\ \dfrac{dI(t)}{dt} = (\varepsilon \chi \gamma_A A(t) - \mu_I)I(t). \end{cases} \tag{3.1}$$

We use the parameter values of Scenario 1 of Lotka-Volterra form in Table 1 for the numerical simulation in Fig. 1.

Table 2

In this table we calculate the positive interior equilibrium of system (1.5) with the parameter values given in Table 1 for Scenario 1–3 of Lotka-Volterra form and for Scenario 1 with Holling's type II functional response.

Equilibrium	Lotka-Volterra form		
	Scenario 1	Scenario 2	Scenario 3
$\bar{A}$	500	500	500
$\bar{\tau}$	158.6998	85.2867	158.6998
$\bar{I}$	16.1142	280.6375	1128.56

Equilibrium	Holling's type II functional response, Scenario 1		
	$\varepsilon = 0.68$	$\varepsilon = 1$	$\varepsilon = 10$
$\bar{A}$	793.6508	526.3158	50.2513
$\bar{\tau}$	250.0769	166.8887	18.7488
$\bar{I}$	0.1118	13.0384	1144.3
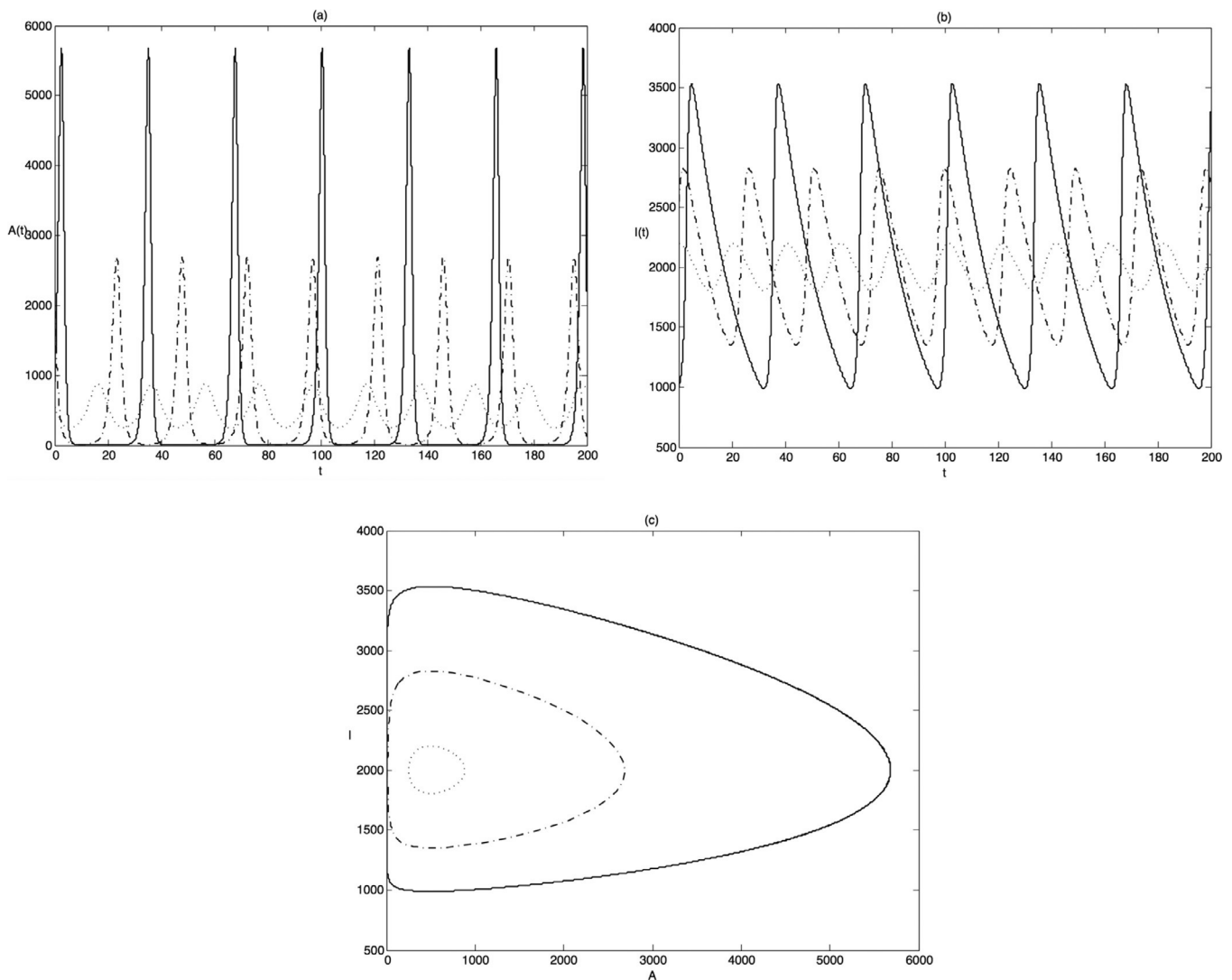
Fig. 1. We plot the simulation of system (3.1) with parameters of Scenario 1 of Lotka-Volterra form in Table 1: $\beta = 2$, $\mu_A = 0.001$, $\gamma_A = 0.001$, $\varepsilon = 1$, $\chi = 0.1$, $\mu_I = 0.05$. The initial values (A_0, I_0) are (550, 2200) (orange), (2000, 2500) (red) and (901.3603, 1000) (blue). Figure (a) and (b) show the adult tree population number $A(t)$ and the nematode population number $I(t)$ respectively. Figure (c) shows the trajectory on the phase plane. The positive interior equilibrium is (500, 1999). (For interpretation of the references to color in this figure legend, the reader is referred to the web version of this article.)

For the parameter values of the other two scenarios of Lotka-Volterra form, the behaviours are similar and we omit those figures here.

3.1.2. Holling's type II functional response – case $\kappa > 0$

We use the parameter values of Scenario 2 with Holling's type II functional response in Table 1 for the numerical simulations of system (1.1) and we get the following trajectory spiraling around the positive interior equilibrium on the phase plane.

We can see from Fig. 2 that after spiraling around the positive equilibrium, the solution follows a line and blow up when the time t goes to infinity. For the remaining sets of parameters corresponding to the other two scenarios in Table 1, similar behaviours happen.

3.2. Simulation with maturation period – case $\tau > 0$

In this section we conduct numerical simulations of system (1.5) with parameter values given in Table 1.

3.2.1. Lotka-Volterra form – case $\kappa = 0$

We set $\kappa = 0$, then system (1.5) is of Lotka-Volterra form.

Scenario 1 (no oscillations): In this part, the parameters of the system are chosen such that in absence of parasite (i.e. when $I_0 = 0$), the number of adult trees $A(t)$ has no oscillations around the positive equilibrium $\bar{A}$ (see Fig. 3).

Now we introduce the nematodes, namely we set $I_0 = 1000$, and we have the following figures.

We find that after the introduction of nematodes, the steady solution $A(t)$ becomes oscillated with a varying amplitude and the maturation period $\tau(t)$ of trees is decreased. But after conducting a longtime simulation, we see that the amplitude of $A(t)$ is gradually stabilized and the trajectory converges to a limit cycle (see Fig. 5). This seems to be related to the periodic solution of the Lotka-Volterra model. Moreover, the maximal value of $A(t)$ is also increased after we introduce the nematodes. However, compared with the Lotka-Volterra model (the blue curve in Fig. 1), the amplitudes of oscillations of both $A(t)$ and $I(t)$ are reduced here.

Scenario 2 (damped oscillations): In this part, the parameters of the system are chosen such that in absence of parasite (i.e. when
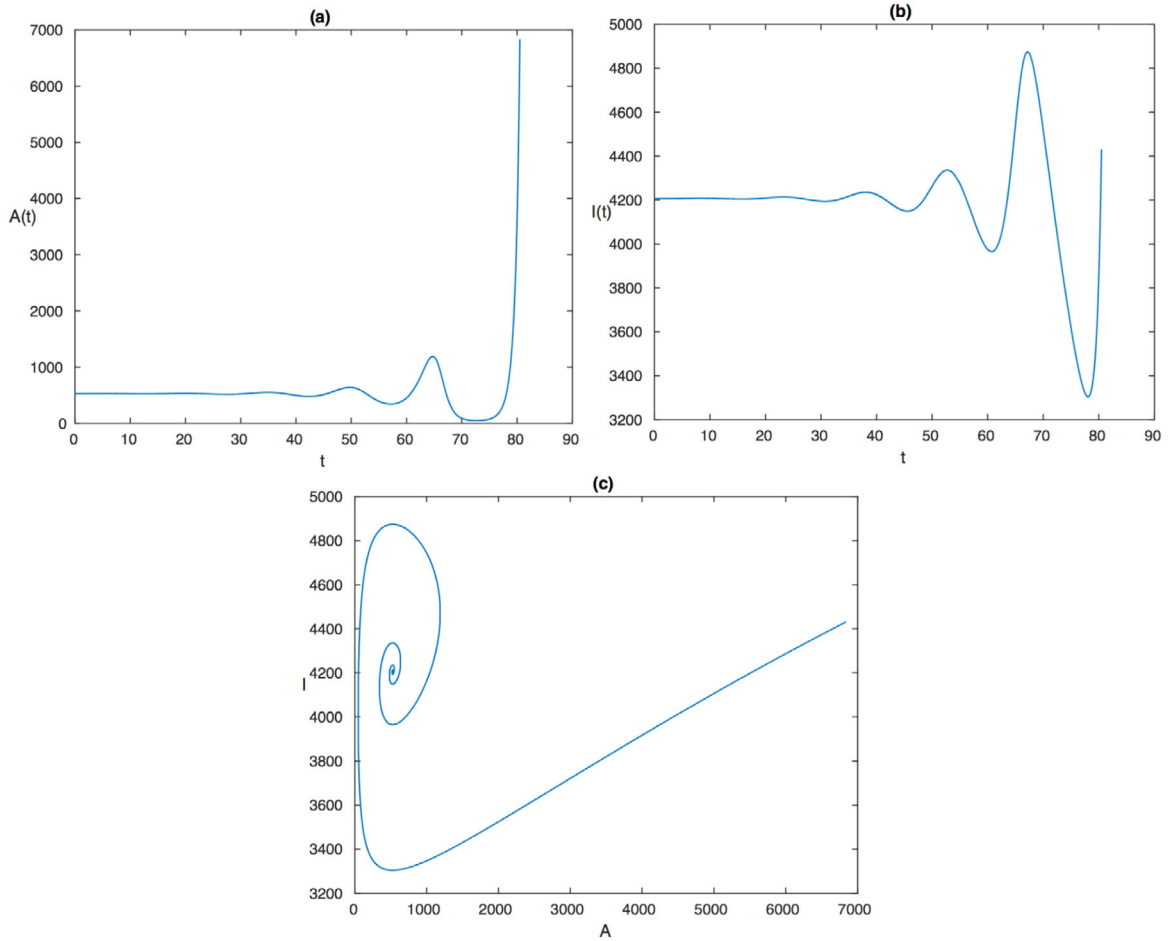
Fig. 2. We plot the simulation of system (1.1) with parameters of Scenario 2 with Holling's type II functional response in Table 1: $\beta = 4$, $\mu_A = 0.0037$, $\gamma_A = 0.001$, $\varepsilon = 1$, $\chi = 0.1$, $\mu_I = 0.05$, $\kappa = 0.0001$. The initial values are $A_0 = 526$, $I_0 = 4206$. Figure (a) and (b) show the adult tree population number $A(t)$ and the nematode population number $I(t)$ respectively. Figure (c) shows the trajectory on the phase plane. A simple calculation shows that the positive interior equilibrium is (526.3158, 4206.6).
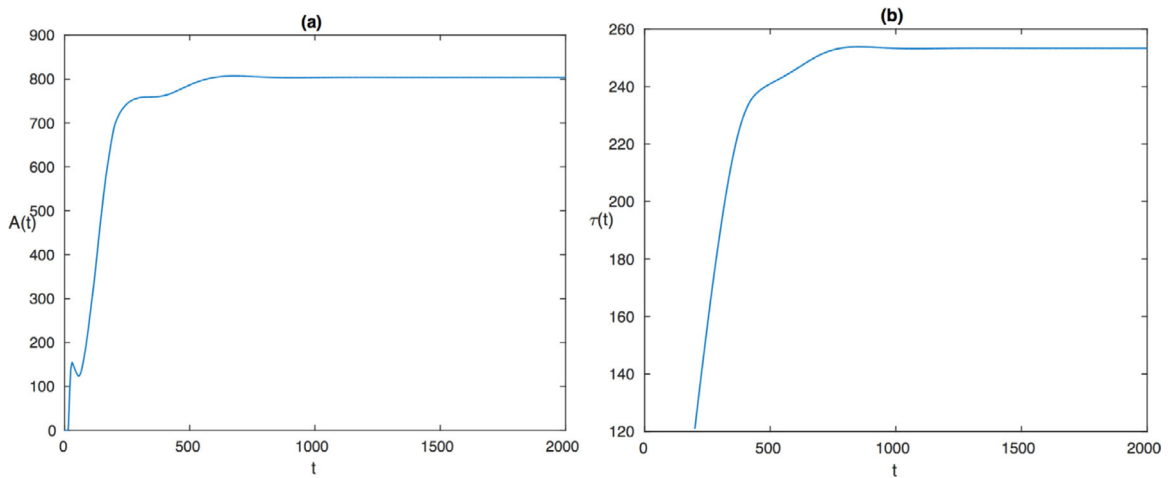
Fig. 3. We plot the simulation of forest model (1.5) with parameters of Scenario 1 of Lotka-Volterra form in Table 1: $\mu_A = 0.001$, $\mu_J = 0.03$, $\beta = 2$, $\delta = 0.1$, $\gamma_A = 0.001$, $\kappa = 0$, $\varepsilon = 1$, $\chi = 0.1$, $\mu_I = 0.05$. We take the distribution of $A(t)$ on the time interval [0, 200] (which comes from the data in Magal and Zhang (2017a)) and $\tau_0 = 121$ as the initial distribution and at the time $t = 200$ we introduce the nematodes with the initial value $I_0 = 0$. Figure (a) shows the adult tree population number $A(t)$ and Figure (b) shows the corresponding time delay $\tau(t)$.
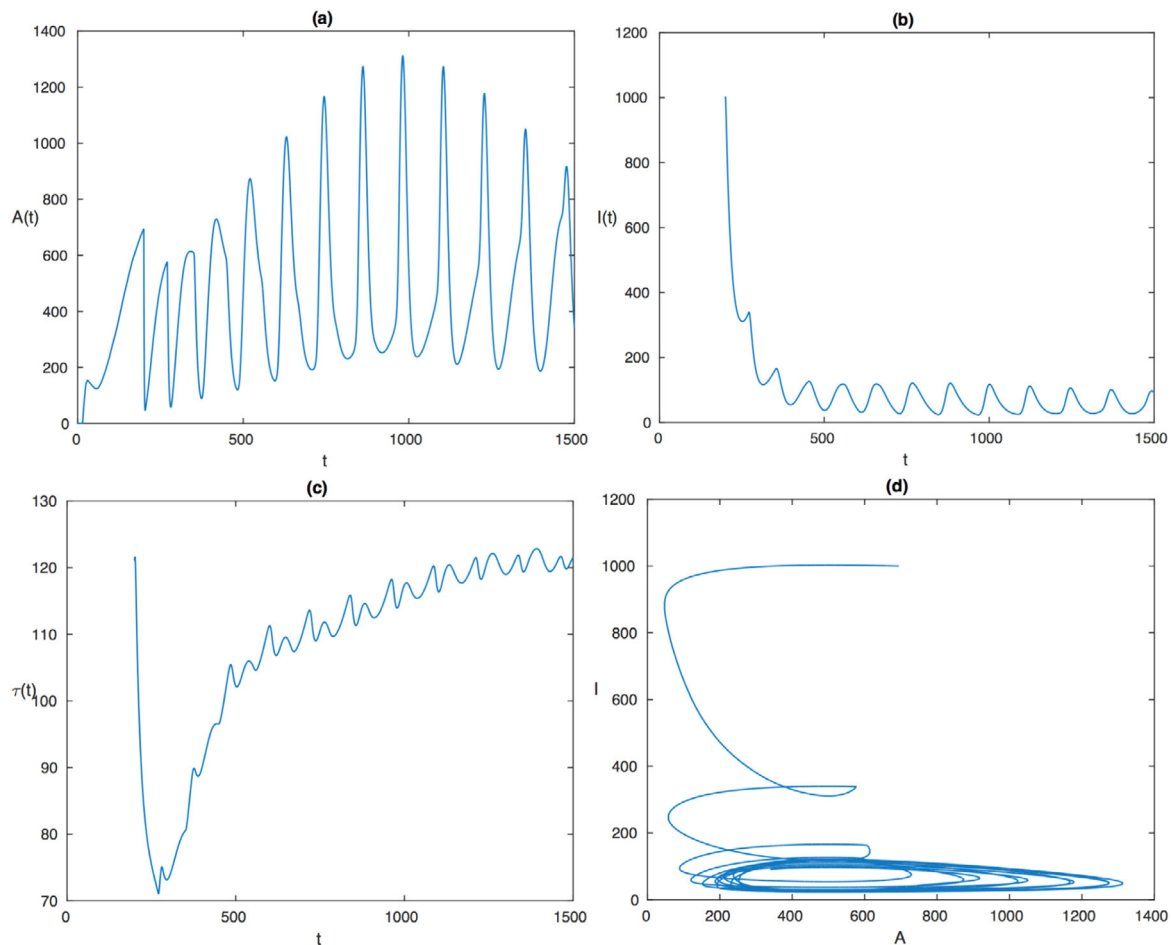
Fig. 4. We plot the simulation of the system (1.5) for Scenario 1 of Lotka-Volterra form in this figure. The parameters and the initial distributions are the same as in Fig. 3 except that at the time $t = 200$ we introduce the nematodes with the initial value $I_0 = 1000$. Figure (a) and (b) show the adult tree population number $A(t)$ and the nematode population number $I(t)$ respectively. Figure (c) shows the corresponding time delay $\tau(t)$ and Figure (d) shows the behaviour on the phase plane.

$I_0 = 0$), the number of adult trees $A(t)$ has some damped oscillations around the positive equilibrium $\bar{A}$ (see Fig. 6).

Now if we fix $I_0 = 1000$, we obtain Fig. 7 .

We can see that the damped oscillating solution $A(t)$ becomes undamped and the amplitude is varying more significantly and more rapidly after we introduce the nematodes. However, the maximal value of $A(t)$ is decreased instead and the maturation period $\tau(t)$ of the trees is also decreased. Compared with the Lotka-Volterra model (the blue curve in Fig. 1), the amplitudes of oscillations of both $A(t)$ and $I(t)$ are also reduced here. On the other hand, compared with Scenario 1, the longtime behaviour is different. The solutions $A(t)$ and $I(t)$ is still periodic but the limit cycle doesn't exist any more (see Fig. 8). The nematode population number $I(t)$ is also increased and the maturation period $\tau(t)$ is decreased compared with Scenario 1.

Scenario 3 (undamped oscillations): In this scenario, the only change is the parameter μ_J, which passes from 0.03 in Scenario 1 to 0.0036 in Scenario 3. As a consequence, in absence of parasite (i.e. when $I_0 = 0$), the number of adult trees $A(t)$ has some undamped oscillations around the positive equilibrium $\bar{A}$ (see Fig. 9).

Now we set $I_0 = 1000$, and we have the following figures.

We can see that after we introduce the nematodes, the periodic solution of $A(t)$ is no longer periodic but with complex oscillations around the positive equilibrium (500, 1128.56) (see Fig. 11 for a detailed view). Compared with the Lotka-Volterra model (the blue curve in Fig. 1), the range of oscillations of both $A(t)$ and $I(t)$ is also

reduced, as the previous two scenarios do. Compared with the previous two scenarios, the range of the oscillation of $A(t)$ is reduced, while the number of nematodes $I(t)$ is largely increased. The maturation delay of the tree population is also increased, which might be the consequence of the large quantity of nematodes slowing down the growth of trees.

3.2.2. Holling's type II functional response – case $\kappa > 0$

Now we turn to the Holling's type II functional response. We will set $\kappa = 0.0001$ in this part.

We start with the numerical simulation of Scenario 1. When $I_0 = 0$, this will be the same result as in Fig. 3, namely the forest model without nematode will have no oscillations. Now we set $I_0 = 1000$ and $\varepsilon = 0.68$, and we get the following results.

We can see that after the introduction of nematodes, the solution $A(t)$ is oscillating and both solutions $A(t)$ and $I(t)$ converge to the positive interior equilibrium (793.6508, 0.1118), and as the equilibrium of $I(t)$ is very small (0.1118), the longtime behaviour is actually still similar to the system without nematode, namely Fig. 3. This is probably due to the small value of the conversion efficiency ε and thus the biomass transformed from trees to nematodes is rather little, which is a disadvantage for the nematodes to persist in a large quantity. Something else happens if we set ε larger (Fig. 13).

With the increase of the conversion efficiency $\varepsilon = 1$, which creates some benefits for the nematode at some level, we get the uniform persistence for both solutions $A(t)$ and $I(t)$, and both so-
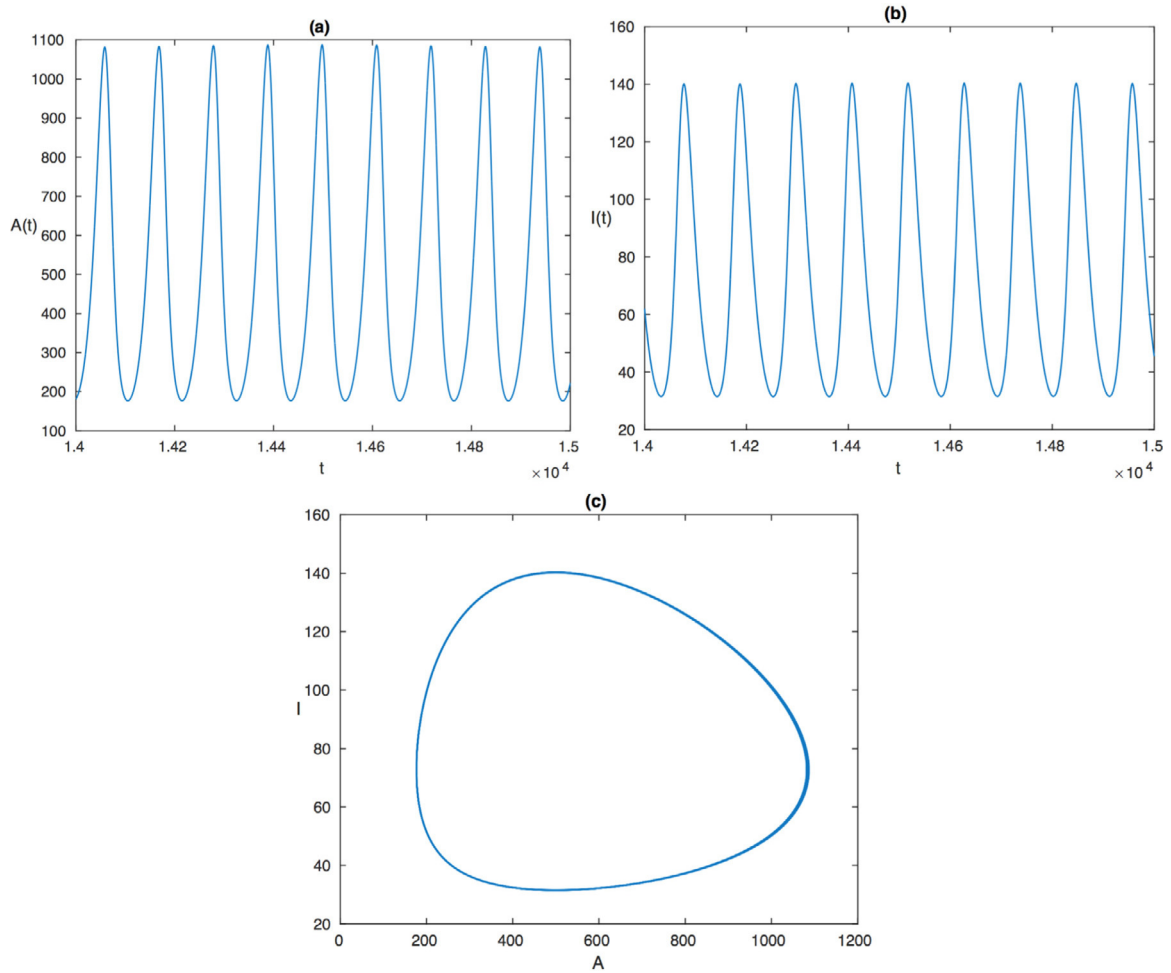
Fig. 5. We plot the longtime behaviour of the simulation in Fig. 4 in the time interval [14,000, 15,000]. The parameters and the initial distribution are the same as in Fig. 4. Figure (a) and (b) show the adult tree population number $A(t)$ and the nematode population number $I(t)$ respectively. Figure (c) shows the trajectory on the phase plane. The trajectory converges to a limit cycle.
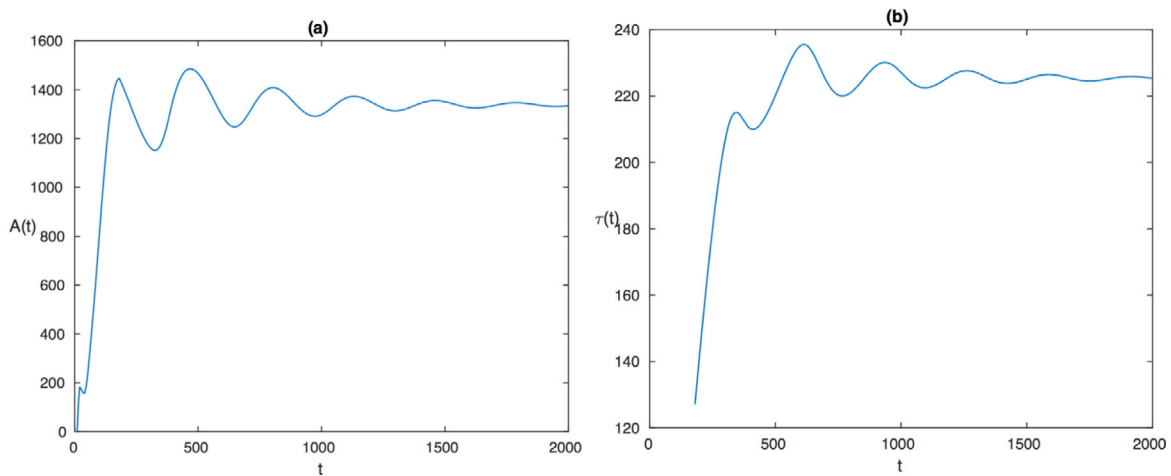
Fig. 6. We plot the simulation of forest model (1.5) with parameters of Scenario 2 of Lotka-Volterra form in Table 1: $\mu_A = 0.0037$, $\mu_J = 0.031$, $\beta = 4$, $\delta = 0.1$, $\gamma_A = 0.001$, $\kappa = 0$, $\varepsilon = 1$, $\chi = 0.1$, $\mu_I = 0.05$. We take the distribution of $A(t)$ on the time interval [0, 180] (which comes from the data in Magal and Zhang (2017a)) and $\tau_0 = 127$ as the initial distribution and at the time $t = 180$ we introduce the nematodes with the initial value $I_0 = 0$. Figure (a) shows the adult tree population number $A(t)$ and Figure (b) shows the corresponding time delay $\tau(t)$.
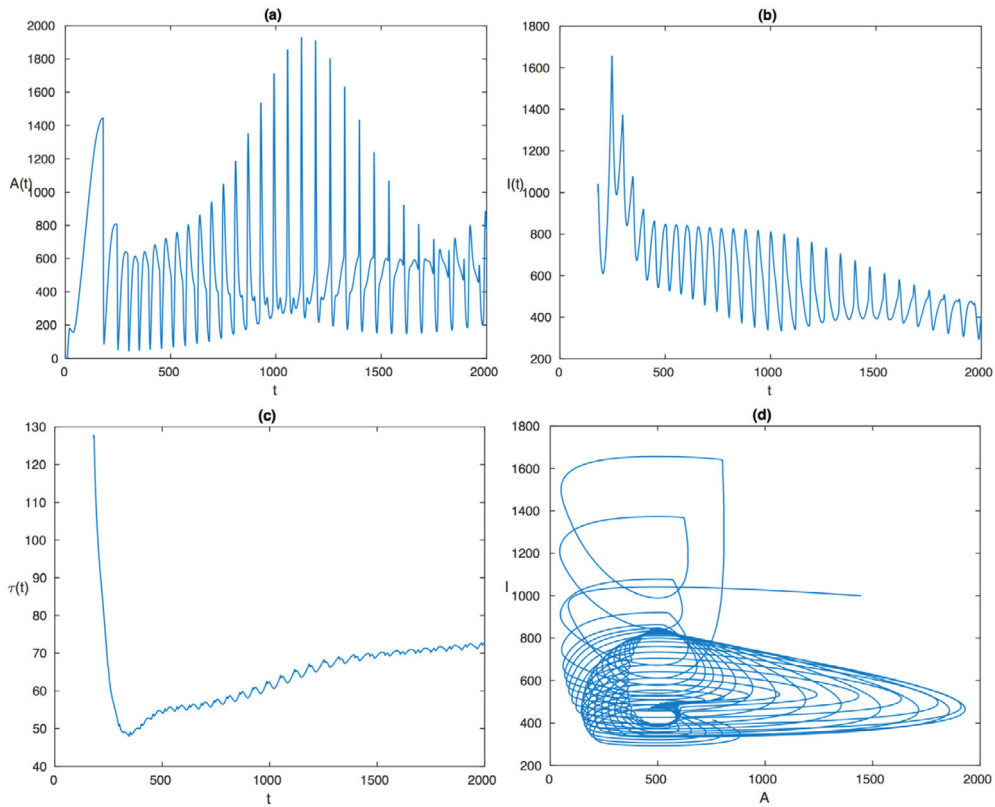
Fig. 7. We plot the simulation of the system (1.5) for Scenario 2 of Lotka-Volterra form in this figure. The parameters and the initial distributions are the same as in Fig. 6 except that at the time $t = 180$ we introduce the nematodes with the initial value $I_0 = 1000$. Figure (a) and (b) show the adult tree population number $A(t)$ and the nematode population number $I(t)$ respectively. Figure (c) shows the corresponding time delay $\tau(t)$ and figure (d) shows the behaviour on the phase plane.
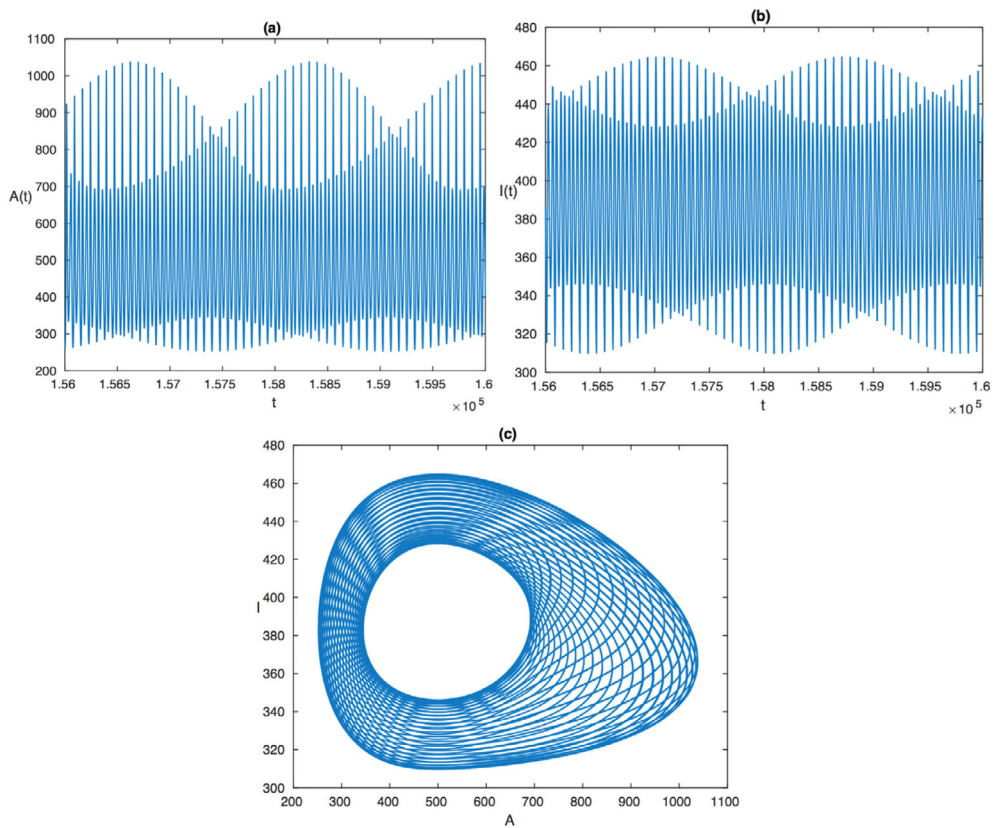
Fig. 8. We plot the longtime behaviour of the simulation in Fig. 7 in the time interval [156,000, 160,000]. The parameters and the initial distribution are the same as in Fig. 7. Figure (a) and (b) show the adult tree population number $A(t)$ and the nematode population number $I(t)$ respectively. Figure (c) shows the trajectory on the phase plane. The trajectory doesn't converge to a limit cycle any more.
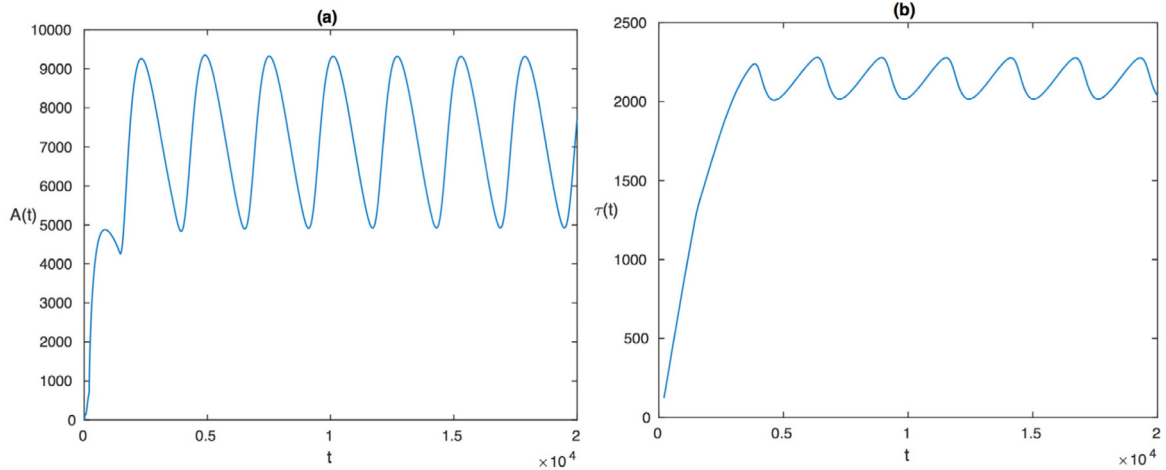
Fig. 9. We plot the simulation of forest model (1.5) with parameters of Scenario 3 of Lotka-Volterra form in Table 1: $\mu_A = 0.001$, $\mu_J = 0.0036$, $\beta = 2$, $\delta = 0.1$, $\gamma_A = 0.001$, $\kappa = 0$, $\varepsilon = 1$, $\chi = 0.1$, $\mu_I = 0.05$. We take the distribution of $A(t)$ on the time interval [0, 200] (which comes from the data in Magal and Zhang (2017a)) and $\tau_0 = 121$ as the initial distribution and at the time $t = 200$ we introduce the nematodes with the initial value $I_0 = 0$. Figure (a) shows the adult tree population number $A(t)$ and Figure (b) shows the corresponding time delay $\tau(t)$.
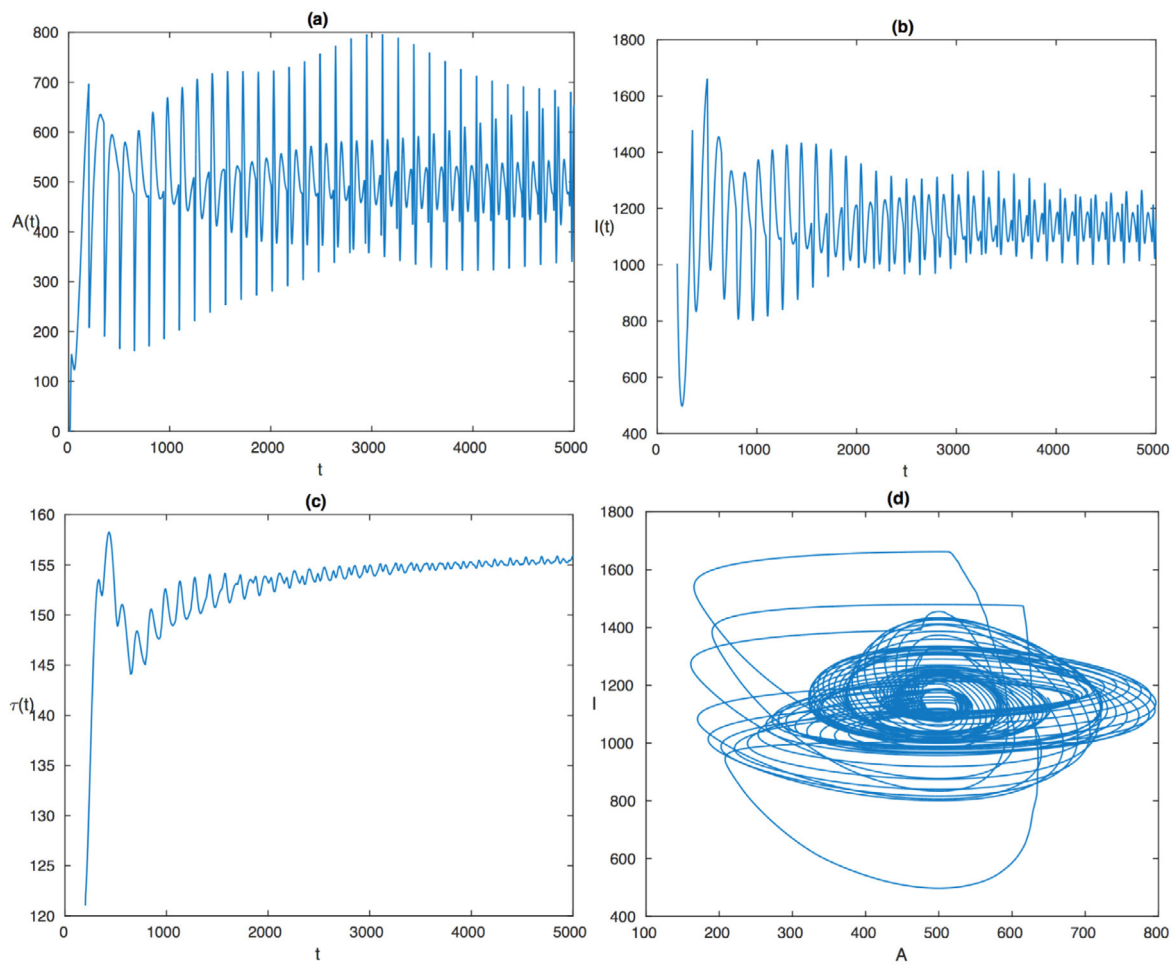
Fig. 10. We plot the simulation of the system (1.5) for Scenario 3 of Lotka-Volterra form in this figure. The parameters and the initial distributions are the same as in Fig. 9 except that at the time $t = 200$ we introduce the nematodes with the initial value $I_0 = 1000$. Figure (a) and (b) show the adult tree population number $A(t)$ and the nematode population number $I(t)$ respectively. Figure (c) shows the corresponding time delay $\tau(t)$ and Figure (d) shows the behaviour on the phase plane.
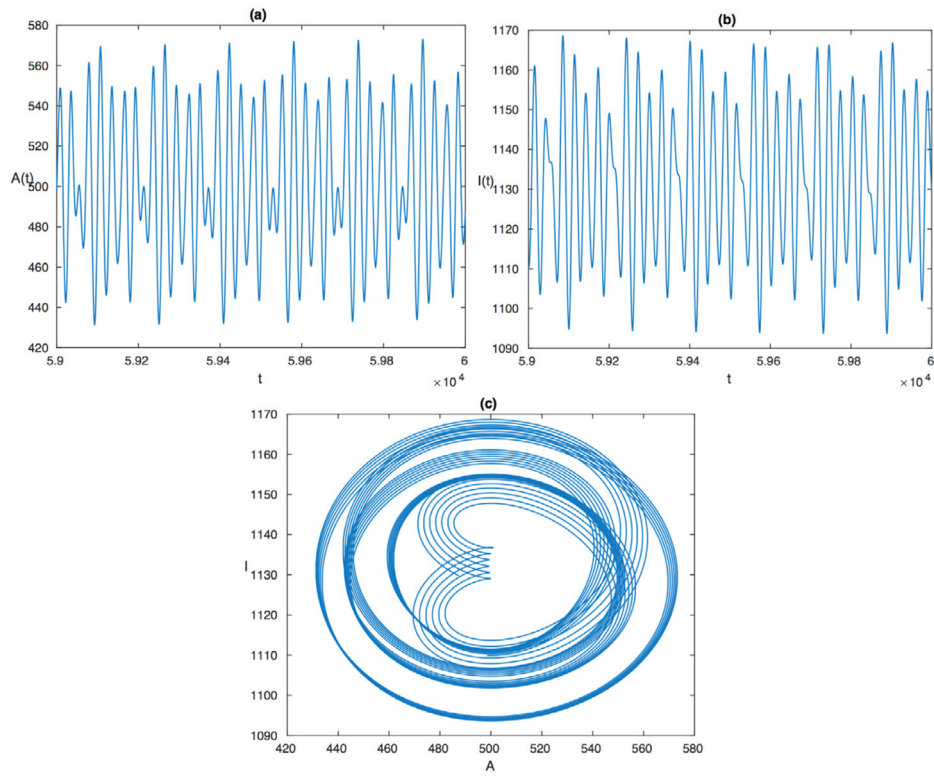
Fig. 11. We plot the longtime behaviour of the simulation in Fig. 10 in the time interval [19000, 20000]. The parameters and the initial distribution are the same as in Fig. 10. Figure (a) and (b) show the adult tree population number $A(t)$ and the nematode population number $I(t)$ respectively. The solutions oscillate around the positive equilibrium (500, 1128.56).
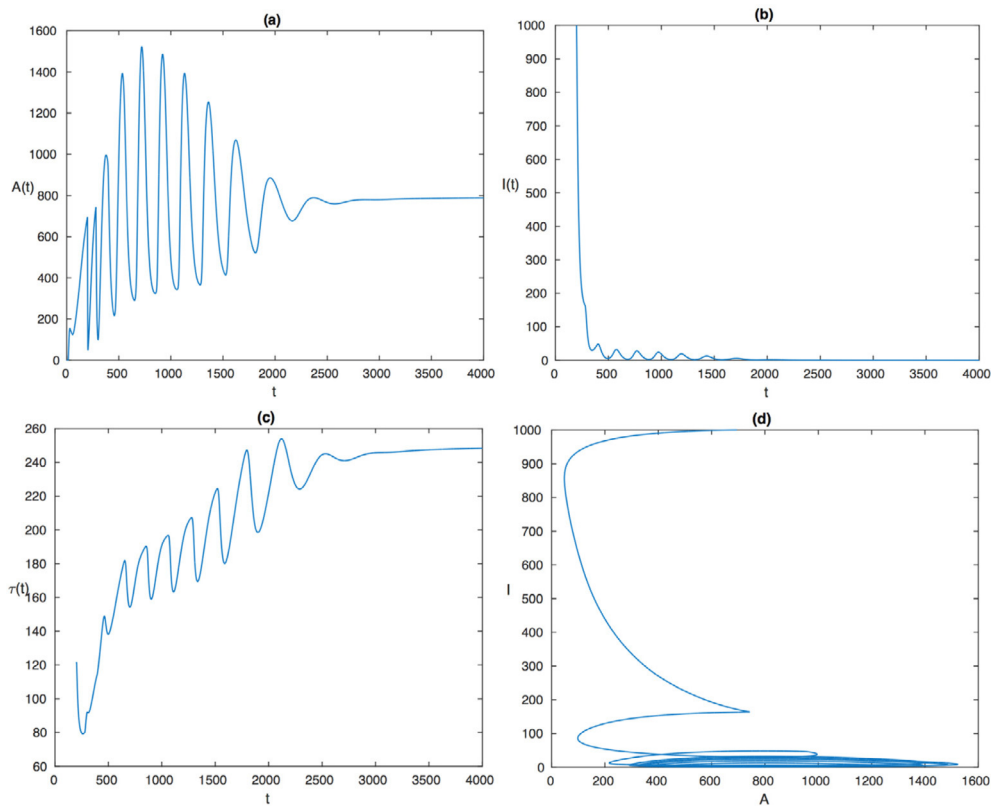
Fig. 12. We plot the simulation of the system (1.5) with parameters of Scenario 1 with Holling's type II functional response in Table 1: $\mu_A = 0.001$, $\mu_J = 0.03$, $\beta = 2$, $\delta = 0.1$, $\gamma_A = 0.001$, $\kappa = 0.0001$, $\varepsilon = 0.68$, $\chi = 0.1$, $\mu_I = 0.05$. We take the distribution of $A(t)$ on the time interval [0, 200] and $\tau_0 = 121$ as the initial distribution and at the time $t = 200$ we introduce the nematodes with the initial value $I_0 = 1000$. Figure (a) and (b) show the adult tree population number $A(t)$ and the nematode population number $I(t)$ respectively. Figure (c) shows the corresponding time delay $\tau(t)$ and Figure (d) shows the behaviour on the phase plane. The solutions $A(t)$ and $I(t)$ converge to the positive interior equilibrium (793.6508, 0.1118) (calculated in Table 2).
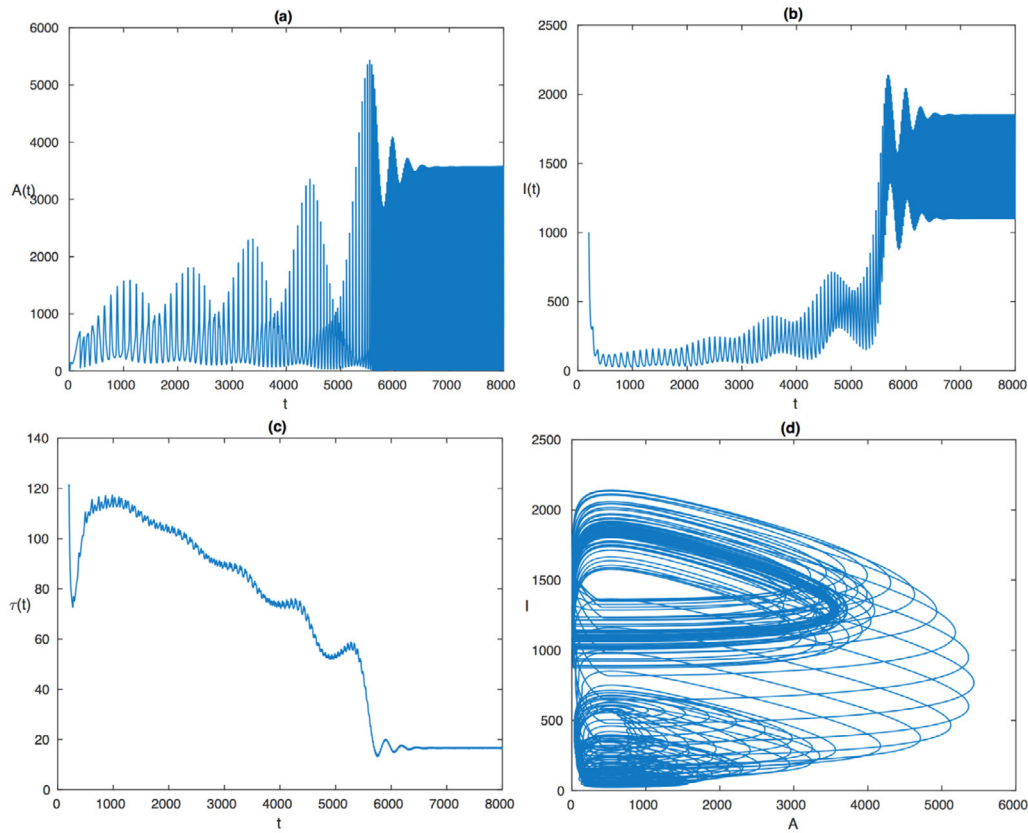
Fig. 13. We plot the simulation of the system (1.5) for Scenario 1 with Holling's type II functional response in this figure. The parameters and initial distributions and the meaning of each figure are the same as in Fig. 12 except that $\varepsilon = 1$. We get oscillating solutions.

lutions exhibit oscillations and the amplitude is largely varying at the beginning and then become stable (actually a long time simulation shows that the "stable" amplitude is still increasing very slowly). This also shows that the positive equilibrium (526.3158, 13.0384) (calculated in Table 2) is not stable. Moreover, the maximal value of $A(t)$ is increased and the maturation period $\tau(t)$ of trees is decreased compared with both the case $\varepsilon = 0.68$ (Fig. 12) and the case $I_0 = 0$ (Fig. 3).

We increase ε again to see what happens next.

When we set $\varepsilon = 10$, no complex oscillations are occurring as in the case $\varepsilon = 1$. The nematode population $I(t)$ reaches a large quantity quickly after it is introduced, due to the high conversion efficiency, and thus the tree population is decreased quickly. After this the tree population oscillates to almost an extinction state but they persist again. This is possibly because the decrease of the tree population leads to the decrease of the nematode population, which creates again a favorable environment for the trees to survive. The solutions both persist in the end and are continuously oscillating with small amplitudes (see Fig. 15).

Remark 3.1. We have run some simulations for the other two scenarios with different values of ε and we find that the system exhibits similar behaviours as Scenario 1. We have also run some simulations for the system with Holling's type III functional response, namely the following system

$$
\begin{cases}
\dfrac{dA(t)}{dt} = f(A(t))\dfrac{\beta A(t - \tau(t))}{f(A(t - \tau(t)))}e^{-\mu_J \tau(t)} - \mu_A A(t) - \dfrac{\gamma_A I(t)A^2(t)}{1 + \kappa A^2(t)}, \\
\displaystyle\int_{t-\tau(t)}^{t} f(A(\sigma))d\sigma = \int_{-\tau_0}^{0} f(A_0(\sigma))d\sigma, \\
\dfrac{dI(t)}{dt} = \left(\dfrac{\varepsilon \chi \gamma_A A^2(t)}{1 + \kappa A^2(t)} - \mu_I\right)I(t),
\end{cases}
$$

and we also have similar behaviours as in the case of Holling's type II functional response.

4. Discussion

Predator-prey systems, or more generally, consumer-resource systems, play a fundamental role in ecology. Different mechanisms between predator and prey will lead to different models with different functional responses (Accolla, 2015; Poggiale, 1998). In this paper, we build a predator-prey model with Lotka-Volterra form competition and Holling's type II functional response and with a state-dependent maturation delay for the prey population. This is based on a forest model, which is constructed in Magal and Zhang (2017a) and in general leads to three scenarios of forest population dynamics (no oscillations, damped oscillations, undamped oscillations), and we incorporate the nematode population into this forest model.

We conduct numerical simulations for the three scenarios and two types of functional responses. First, with Lotka-Volterra form competition, after we introduce a non-null state-dependent delay to describe the maturation period of the tree population, the solutions start with complex oscillations and then become regular,
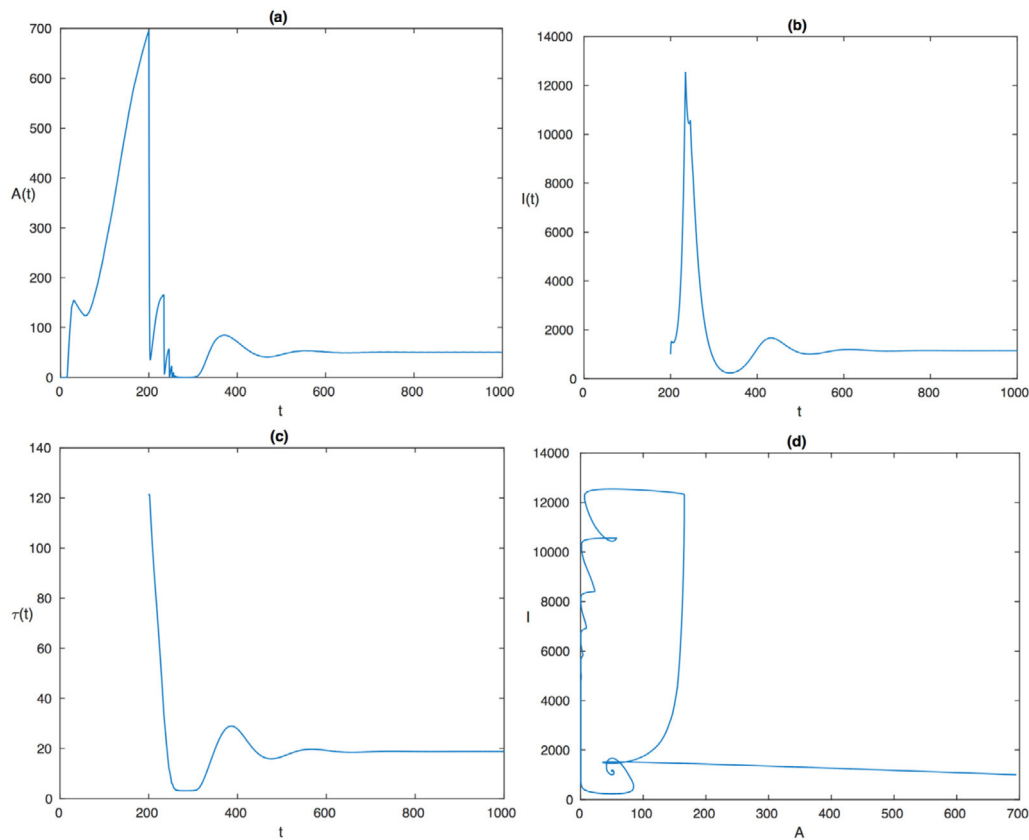
Fig. 14. We plot the simulation of the system (1.5) for Scenario 1 with Holling's type II functional response in this figure. The parameters and initial distributions and the meaning of each figure are the same as in Fig. 12 except that $\varepsilon = 10$. We get slightly oscillating solutions.
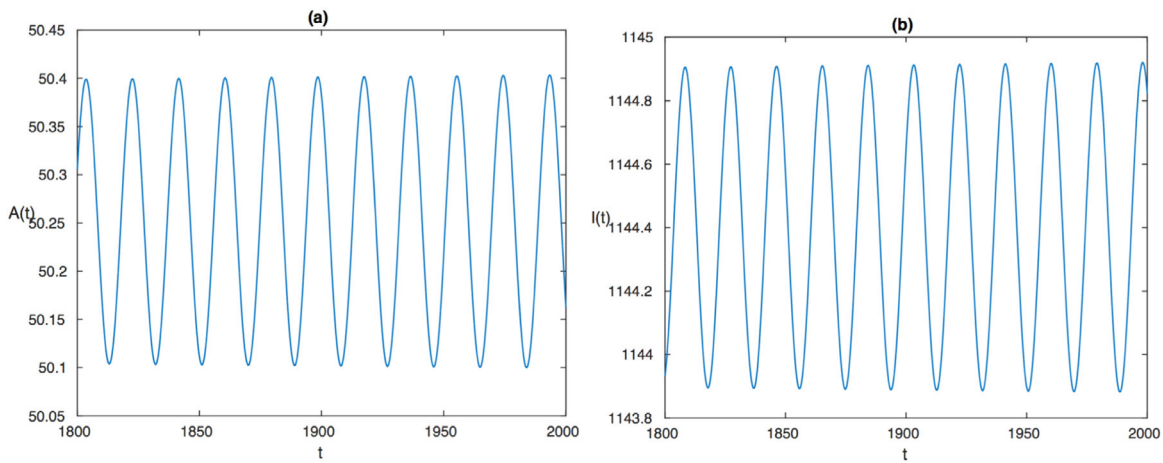
Fig. 15. We plot the simulation of the solution $A(t)$ and $I(t)$ in Fig. 14 in the time interval [1800, 2000] in this figure. The solutions are oscillating with small amplitude.

that is to say, the solutions converge to a limit cycle again in Scenario 1 and undergo some superposition of two oscillations in Scenario 2 and 3. Moreover, for all the three scenarios, the two solutions still persist, only with a reduced amplitude of oscillations compared with the corresponding system without the maturation delay (system (3.1)).

With Holling's type II functional response, the system is perturbed vastly after the introduction of the maturation delay, and the previous unbounded solution becomes bounded. But this also depends on the rate of conversion efficiency of the energy from prey to predator. When this rate is too low, the predator can't persist, and thus the system has similar behaviours as the case when

there is no predator. If this rate of conversion efficiency is rather high, the system risks of going to extinction for both predator and prey but it adapts itself to a persisting state again.

Now, from another point of view, after we introduce the nematodes into the forest, no matter which type of functional response it is, we see that the solution $A(t)$ which doesn't oscillate before (Scenario 1) starts to oscillate, and which has oscillations (damped or periodic) before (Scenario 2 and 3) undergoes undamped oscillation after the introduction of nematodes.

We might also notice that after the introduction of nematodes, the maturation delay $\tau(t)$ is also reduced for all three scenarios and two types of functional responses. That is because with the
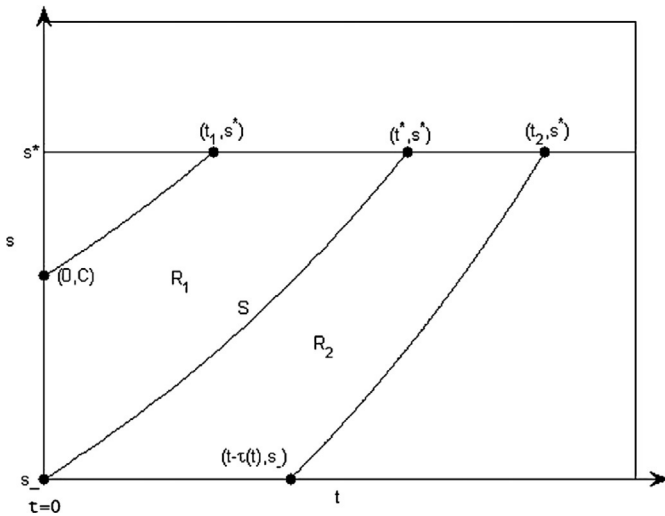
Fig. 16. In this figure we present the characteristic curves (A.2).

introduction of nematodes $I(t)$, the adult tree population number $A(t)$ is affected, then by the second equation of system (1.5), which is used to solve $\tau(t)$, this maturation delay will also be affected. Moreover, we need to point out that the unit of the solution $\tau(t)$ is "year". Then there seems to be something unrealistic here in that in some cases, the equilibrium of $\tau(t)$ is more than 100, which means that it needs more that 100 years for a tree to grow mature. Actually, the delay $\tau(t)$ is used to describe the time needed for the trees to grow to be adults, and also, to be able to produce new generations in the middle of a forest. This means that the trees can be affected by the other surrounding trees, then not so many trees can survive to be able to produce an adult tree and thus on average it takes a longer time for them to grow.

Appendix A. Derivation of the state-dependent delay differential equation

We can transform the system (1.3) into a state-dependent delay differential equation using the method in Magal and Zhang (2017a); Smith (1993, 1994). Differentiating the following formula

$$A(t) = \int_{s^*}^{+\infty} u(t,s)\, ds$$

with respect to t, we have

$$\begin{aligned}
\frac{dA(t)}{dt} &= \int_{s^*}^{+\infty} \partial_t u(t,s)\, ds \\
&= -f(A(t)) \int_{s^*}^{+\infty} \partial_s u(t,s)\, ds - \int_{s^*}^{+\infty} \left[\mu(s) + \frac{\gamma(s)I(t)}{1+\kappa A(t)}\right] u(t,s)\, ds \quad \text{(A.1)}\\
&= f(A(t))u(t,s^*) - \int_{s^*}^{+\infty} \left[\mu(s) + \frac{\gamma(s)I(t)}{1+\kappa A(t)}\right] u(t,s)\, ds.
\end{aligned}$$

Next we deal with the term $u(t, s^*)$. The characteristic curves for the first equation in (1.3) are (shown in Fig. 16)

$$\frac{ds(t)}{dt} = f(A(t)). \quad \text{(A.2)}$$

Then we will have the following representation of s

$$s(t) = C + \int_0^t f(A(\sigma))\, d\sigma. \quad \text{(A.3)}$$

Suppose t^* is the time when juveniles present at time 0 become adults, namely

$$\int_0^{t^*} f(A(\sigma))\, d\sigma = s^* - s_-.$$

We can see that the curve

$$S = \left\{(t,s): \ 0 \le t \le t^*, \ s = s_- + \int_0^t f(A(\sigma))\, d\sigma\right\}$$

divides the strip $[0, +\infty) \times [s_-, s^*]$ into two parts R_1 and R_2. Assuming that $s - s_- \le \int_0^t f(A(\sigma))\, d\sigma$, then we can find $T(t, s) \ge 0$ such that

$$\int_{t-T(t,s)}^t f(A(\sigma))\, d\sigma = s - s_-$$

in the region R_2, so it denotes the time it takes for a juvenile to grow to size s at time t from the minimal size s_-. Replacing s in $u(t, s)$ with (A.3), we can compute formally as follows, assuming that u is a C^1-function:

$$\begin{aligned}
\frac{d}{dt}u &\left(t, C + \int_0^t f(A(\sigma))\, d\sigma\right) \\
&= \partial_t u\left(t, C + \int_0^t f(A(\sigma))\, d\sigma\right) \\
&\quad + f(A(t)) \partial_s u\left(t, C + \int_0^t f(A(\sigma))\, d\sigma\right) \\
&= -\left[\mu\left(C + \int_0^t f(A(\sigma))\, d\sigma\right) + \frac{\gamma\left(C + \int_0^t f(A(\sigma))\, d\sigma\right)I(t)}{1+\kappa A(t)}\right] \\
&\quad u\left(t, C + \int_0^t f(A(\sigma))\, d\sigma\right).
\end{aligned}$$

This is a separable ODE with respect to t. Integration of this equation, and by using the initial distribution and the boundary condition, we obtain the following expression of $u(t, s)$

$$\begin{aligned}
u(t,s) = &\left\{ u_0\left(s - \int_0^t f(A(\sigma))\, d\sigma\right) \exp\left\{-\int_0^t \left[\mu\left(s - \int_0^t f(A(\sigma))\, d\sigma + \int_0^l f(A(\sigma))\, d\sigma\right)\right.\right.\right. \\
&\left.\left.\left. + \frac{\gamma\left(s - \int_0^t f(A(\sigma))\, d\sigma + \int_0^l f(A(\sigma))\, d\sigma\right)I(l)}{1+\kappa A(l)}\right]dl\right\}, \text{ if } s \ge s_- + \int_0^t f(A(\sigma))\, d\sigma, \\
&\frac{\beta A(t-T(t,s))}{f(A(t-T(t,s)))} \exp\left\{-\int_{t-T(t,s)}^t \left[\mu\left(s_- + \int_{t-T(t,s)}^l f(A(\sigma))\, d\sigma\right)\right.\right. \\
&\left.\left. + \frac{\gamma\left(s_- + \int_{t-T(t,s)}^l f(A(\sigma))\, d\sigma\right)I(l)}{1+\kappa A(l)}\right]dl\right\}, \text{ if } s \le s_- + \int_0^t f(A(\sigma))\, d\sigma. \quad \text{(A.4)}
\end{aligned}$$

Whenever $s^* - s_- \le \int_0^t f(A(\sigma))\, d\sigma$, we can specifically define $\tau(t) := T(t, s^*)$ as the solution of

$$\int_{t-\tau(t)}^t f(A(\sigma))\, d\sigma = s^* - s_-. \quad \text{(A.5)}$$

Actually the term $\tau(t) = T(t, s^*)$ represents the maturation period of one individual.

We now assume

$$\mu(s) = \begin{cases} \mu_A > 0, & \text{if } s \ge s^*, \\ \mu_J > 0, & \text{if } s < s^*, \end{cases} \qquad \gamma(s) = \begin{cases} \gamma_A \ge 0, & \text{if } s \ge s^*, \\ \gamma_J \ge 0, & \text{if } s < s^*. \end{cases}$$

Then the third equation of (1.3) becomes

$$\frac{dI(t)}{dt} = \left[\frac{\varepsilon\chi}{1+\kappa A(t)}(\gamma_A A(t) + \gamma_J J(t)) - \mu_I\right]I(t). \quad \text{(A.6)}$$

When $s = s^*$, we have for $t \in [0, t^*]$,

$$u(t, s^*) = u_0\left(s^* - \int_0^t f(A(\sigma))\, d\sigma\right) e^{-\mu_J t - \gamma_J \int_0^t \frac{I(l)}{1+\kappa A(l)}\, dl},$$

and for $t > t^*$,

$$u(t, s^*) = \frac{\beta A(t-\tau(t))}{f(A(t-\tau(t)))} e^{-\mu_J \tau(t) - \gamma_J \int_{t-\tau(t)}^t \frac{I(l)}{1+\kappa A(l)}\, dl}.$$

Replacing $u(t, s*)$ back in (A.1) for $t > t*$, we get the equation of $A(t)$ in (1.4):

$$\frac{dA(t)}{dt} = \frac{f(A(t))}{f(A(t - \tau(t)))} e^{-\mu_J \tau(t) - \gamma_J \int_{t-\tau(t)}^{t} \frac{I(l)}{1+\kappa A(l)} dl} \beta A(t - \tau(t)) \\ - \mu_A A(t) - \gamma_A \frac{A(t)}{1 + \kappa A(t)} I(t).$$
(A.7)

Set $\gamma_J = 0$. Then when $t > t*$, system (1.3) is transformed into system (1.5).

Appendix B. Derivation of the numerical scheme

We will give the numerical scheme in this appendix for the system (1.5). First we can rewrite system (1.5) in the following form:

$$\begin{cases} A'(t) = F(A(t), I(t), \tau(t), A(t - \tau(t))), \\ \int_{t-\tau(t)}^{t} f(A(\sigma)) d\sigma = s^* - s_-, \\ I'(t) = G(A(t), I(t)). \end{cases}$$
(B.1)

where

$$F(A_0, I, \tau, A_{-\tau}) := \frac{f(A_0)}{f(A_{-\tau})} e^{-\mu_J \tau} \beta A_{-\tau} - \mu_A A_0 - \gamma_A \frac{A_0}{1 + \kappa A_0} I$$

and

$$G(A, I) := \left(\frac{\varepsilon \chi \gamma_A A}{1 + \kappa A} - \mu_I \right) I.$$

First we give a derivation of the numerical scheme of the computation of $\tau(t)$. From the second equation of (B.1) we have

$$\int_{t-\tau(t)}^{t} f(A(\sigma)) d\sigma = \int_{t+\Delta t - \tau(t+\Delta t)}^{t+\Delta t} f(A(\sigma)) d\sigma,$$

which is equivalent to

$$\int_{t-\tau(t)}^{t+\Delta t} f(A(\sigma)) d\sigma + \int_{t+\Delta t}^{t} f(A(\sigma)) d\sigma \\ = \int_{t+\Delta t - \tau(t+\Delta t)}^{t-\tau(t)} f(A(\sigma)) d\sigma + \int_{t-\tau(t)}^{t+\Delta t} f(A(\sigma)) d\sigma.$$

So

$$\int_{t+\Delta t}^{t} f(A(\sigma)) d\sigma = \int_{t+\Delta t - \tau(t+\Delta t)}^{t-\tau(t)} f(A(\sigma)) d\sigma.$$
(B.2)

Assume Δt is small enough, then $f(A(\sigma))$ can be seen as a constant function on the interval $[t, t + \Delta t]$ and $[t - \tau(t), t + \Delta t - \tau(t + \Delta t)]$. Thus we approximate $f(A(\sigma))$ by $f(A(t))$ in the first integral and by $f(A(t - \tau(t)))$ in the second integral in (B.2), and we have the following approximation

$$\Delta t f(A(t)) = (\Delta t - \tau(t + \Delta t) + \tau(t)) f(A(t - \tau(t))),$$

and

$$\tau(t + \Delta t) = \tau(t) + \Delta t \left(1 - \frac{f(A(t))}{f(A(t - \tau(t)))} \right).$$

Then the numerical scheme used in this article will be

$$\begin{cases} A(t + \Delta t) = \Delta t F(A(t), I(t), \tau(t), A(t - \tau(t))) + A(t), \\ \tau(t + \Delta t) = \Delta t \left(1 - \frac{f(A(t))}{f(A(t - \tau(t)))} \right) + \tau(t), \\ I(t + \Delta t) = \Delta t G(A(t), I(t)) + I(t). \end{cases}$$
(B.3)

It remains to find a numerical approximation to calculate $A(t - \tau(t))$, namely the past value of A at time $t - \tau(t)$ in the above approximation, which might not be given in the previous calculation because $t - \tau(t)$ might not be in our discretized sequence of time for the simulation. In order to determine this value, we use the method of linear interpolation. First we determine the time interval $[t_n, t_{n+1}]$ (with $t_n := n\Delta t$ for some integer $n \in \mathbb{Z}$) to which the time $t - \tau(t)$ belongs, then we use the following linear interpolation

$$A(t - \tau(t)) \approx A(t_n) + (t - \tau(t) - t_n) \frac{A(t_{n+1}) - A(t_n)}{t_{n+1} - t_n}$$
(B.4)

to get the approximation of the value $A(t - \tau(t))$. This will be more accurate than the rough approximation of using just $A(t_n)$ or $A(t_{n+1})$.

References

Accolla, C., 2015. Modélisation de la formation des bancs de poissons: Évaluation des conséquences de l'agrégation des individus dans un système proies-prédateurs à différentes échelles. Thèse de doctorat, Aix-Marseille Université.

Dawes, J., Souza, M., 2013. A derivation of Holling's type I, II and III functional responses in predator-prey systems. J. Theor. Biol. 327, 11–22.

Gruffudd, H., Jenkins, T., Evans, F., 2016. Using an evapo-transpiration model (ETPN) to predict the risk and expression of symptoms of pine wilt disease (PWD) across Europe. Biol. Invas. 18, 2823–2840.

Holland, J., DeAngelis, D., 2009. Consumer-resource theory predicts dynamic transitions between outcomes of interspecific interactions. Ecol. Lett. 12, 1357–1366.

Holland, J., DeAngelis, D., 2010. A consumer-resource approach to the density-dependent population dynamics of mutualism. Ecology 91, 1286–1295.

Holling, C., 1959. The components of predation as revealed by a study of small–mammal predation of the European pine sawfly. Can. Entomol. 91 (5), 293–320.

Holling, C., 1959. Some characteristics of simple types of predation and parasitism. Can. Entomol. 91 (7), 385–398.

Kazarinoff, N., Driessche, P., 1978. A model predator-prey system with functional response. Math. Biosci. 39, 125–134.

Koutroumpa, F., 2007. Biologie et phylogéographie de *Monochamus galloprovincialis* (Coleoptera, Cerambycidae) vecteur du nématode du pin en Europe. Thèse de doctorat, Université d'Orléans.

Lafferty, K., DeLeo, G., Briggs, C., Dobson, A., Gross, T., Kuris, A., 2015. A general consumer-resource population model. Science 349 (6250), 854–857.

Lotka, A., 1925. Elements of Physical Biology. The Williams and Wilkim Co, Baltimore, MD.

Magal, P., Zhang, Z., 2017. Competition for light in a forest population dynamic model: from computer model to mathematical model. J. Theor. Biol. 419, 290–304.

P. Magal, Z. Zhang, A system of state-dependent delay differential equation modelling forest growth I: existence and uniqueness of the solutions (in preparation).

MacArthur, R., 1972. Geographical Ecology. Harper and Row, New York.

May, R., 1972. Limit cycles in predator-prey communities. Science 177, 900–902.

Mota, M., Braasch, H., Bravo, M., Penas, A., Burgermeister, W., Metge, K., Sousa, E., 1999. First report of *Bursaphelenchus xylophilus* in Portugal and in Europe. Nematology 1 (7–8), 727–734.

Mota, M., Futai, K., Vieira, P., 2009. Pine Wilt Disease and the Pinewood Nematode, *Bursaphelenchus xylophilus*, Integrated Management of Fruit Crops Nematodes. Springer Netherlands, pp. 253–274.

Mota, M., Vieira, P., 2008. Pine Wilt Disease in Portugal, Pine Wilt Disease. Springer, Japan, pp. 33–38.

Poggiale, J., 1998. Predator-prey models in heterogeneous environment: emergence of functional response. Math. Comput. Model. 27 (4), 63–71.

Rodrigues, J., 2008. National Eradication Programme for the Pinewood Nematode, Pine Wilt Disease: A Worldwide Threat to Forest Ecosystems. Springer, Netherlands, pp. 5–14.

Rosenzweig, M., MacArthur, R., 1963. Graphical representation and stability conditions of predator prey interactions. Am. Nat. 97, 209–223.

Smith, H.L., 1993. Reduction of structured population models to threshold-type delay equations and functional differential equations: a case study. Math. Biosci. 113, 1–23.

Smith, H.L., 1994. A structured population model and a related functional differential equation: global attractors and uniform persistence. J. Dyn. Differ. Equ. 6 (1), 71–99.

Sousa, E., Bravo, M., Pires, J., Naves, P., Penas, A., Bonifácio, L., Mota, M., 2001. *Bursaphelenchus xylophilus* (Nematoda; Aphelenchoididae) associated with *Monochamus galloprovincialis* (Coleoptera; Cerambycidae) in Portugal. Nematology 3 (1), 89–91.

Sousa, E., Naves, P., Bonifácio, L., Bravo, M., Penas, A., Pires, J., Serr ao, M., 2002. Preliminary survey for insects associated with *Bursaphelenchus xylophilus* in Portugal. EPPO Bull. 32 (3), 499–502.

Vicente, C., Espada, M., Vieira, P., Mota, M., 2012. Pine wilt disease, a threat to European forestry. Eur. J. Plant Pathol. 133 (1), 89–99.

Volterra, V., 1927. Variazioni e fluttuazioni del numero d'individui in specie animali conviventi, C. Ferrari.

Volterra, V., 1928. Variations and fluctuations of the number of individuals in animal species living together. Journal du conseil/conseil permanent international pour l'exploration de la mer 3 (1), 3–51.

Webb, G., 2008. Population models structured by age, size, and spatial position. Structured Population Models in Biology and Epidemiology, Lecture Notes in Mathematics, vol. 1936. Springer-Verlag, Berlin/New York, pp. 1–49.